Available online at www.sciencedirect.com
ScienceDirect
China Particuology 5 (2007) 162–168
China Particuology
www.elsevier.com/locate/cpart

Dextran-modified iron oxide nanoparticles

Jiří Hradil, Alexander Pisarev, Michal Babič, Daniel Horák *

Institute of Macromolecular Chemistry, Academy of Sciences of the Czech Republic Heyrovsky Sq. 2, 162 06 Prague, Czech Republic

Received 6 September 2006; accepted 25 January 2007

Abstract

Dextran-modified iron oxide nanoparticles were prepared by precipitation of Fe(II) and Fe(III) salts with ammonium hydroxide by two methods. Iron oxide was precipitated either in the presence of dextran solution, or the dextran solution was added after precipitation. In the second method, the iron oxide particle size and size distribution could be controlled depending on the concentration of dextran in the solution. The nanoparticles were characterized by size-exclusion chromatography, transmission electron microscopy and dynamic light scattering. Optimal conditions for preparation of stable iron oxide colloid particles were determined. The dextran/iron oxide ratio 0–0.16 used in precipitation of iron salts can be recommended for synthesis of nanoparticles suitable for biomedical applications, as the colloid does not contain excess dextran and does not coagulate.

Keywords: Iron oxide; Nanoparticles; Dextran; Size-exclusion chromatography; Particle size

1. Introduction

Iron oxide nanoparticles find increasing applications especially in medicinal diagnostics, as contrast agents in magnetic resonance imaging of tumours and soft tissues, for cell labelling, etc. (Gupta & Gupta, 2005). In drug targeting, they are used for tumour therapy or cardiovascular disease (Neuberger, Schöpf, Hofmann, Hofmann, & von Rechenberg, 2005); detoxification of blood toxins was also proposed (Kaminski & Rosengart, 2005).

Many methods have been described for the synthesis of iron oxides, mainly maghemite and magnetite nanoparticles (Cabasso & Yuan, 1996), as they exhibit superparamagnetic properties which are necessary to prevent particle aggregation. They include size reduction methods, thermal decomposition of iron carbonyl, laser-induced reaction and ablation, synthesis of organometallics, magnetotactic bacteria and chemical coprecipitation techniques. The size-reduction method is based on grinding commercial magnetite powder (ca. 30 μm in size) in a ball mill in the presence of a liquid carrier (e.g., heptane) and dispersant (e.g., oleic acid) (Papel, 1965). Fine ferromagnetic particles can also be prepared by thermal decomposition of metal carbonyls in gases of various organic liquids or in vacuum (Griffiths, O'Horo, & Smith, 1979; Syirkin & Polushina, 1967). Chemical coprecipitation produces water-based dispersions of iron oxides, the so-called magnetic fluids. Finely dispersed iron oxides are coprecipitated from a solution of Fe(II) and Fe(III) salts and the precipitate is washed with distilled water (Jolivet, Massart, & Fruchart, 1983; Massart, 1981). The advantage of alkaline coprecipitation compared to the previous methods consists in its simplicity. In contrast to grinding methods, coprecipitation provides a narrow size distribution and the yield is higher. Hydrophilic polymers, such as dextran (Molday, 1984), poly(vinyl alcohol) (Chastellain, Petri, & Hofmann, 2004) and poly(ethylene glycol) are often present during the precipitation in order to control particle size and agglomeration and to facilitate intravenous administration.

Iron oxide nanoparticles usually display a broad particle size distribution. Size should be in the 3–10 nm range to impart superparamagnetic properties (Bonnemain, 1998). Particle size and particle size distribution have a strong effect on physical properties of colloidal dispersions. For many systems, the measurement of average particle size by the two most commonly used methods, electron microscopy or dynamic light scattering, is not sufficient. In this context, chromatography is very useful for nanoparticle characterization. In comparison with other meth-

* Corresponding author. Tel.: +420 296 809 260; fax: +420 296 809 410.
E-mail address: horak@imc.cas.cz (D. Horák).

1672-2515/$ – see front matter © 2007 Chinese Society of Particuology and Institute of Process Engineering, Chinese Academy of Sciences. Published by Elsevier B.V.All rights reserved.
doi:10.1016/j.cpart.2007.01.003

ods, such as transmission electron microscopy or light scattering, chromatographic techniques allow to determine concentration changes. They include size exclusion and hydrodynamic chromatography (Williams, Varela, Meehan, & Tribe, 2002) and field flow fractionation. Hydrodynamic chromatography (separation in interparticle channels) was recently miniaturized on chip (Chmela, Tijssen, Blom, Gardeniers, & van den Berg, 2002). Field flow fractionation (Rheinlander, Roessner, Weitschies, & Semmler, 2000), which makes it possible to fractionate samples from few nanometres to hundred micrometers in size, includes several modifications, such as asymmetric (Johann, 1998), frit-inlet asymmetric (Moon, 2001), sedimentation (Anger, Caldwell, Mehnert, & Muller, 1999), micro-thermal (Janča, Ananieva, Menshikova, & Evseeva, 2004; Janča, Berneron, & Boutin, 2003) and frontal (Janča & Strnad, 2004). Size-exclusion chromatography (SEC) is a well-established method for separation of macromolecules in solution according to their size (Liu & Wei, 2004; Wei, Liu, & Wang, 1999). Nanoparticles were also separated on monolithic chromatography columns (Kramberger, Glover, & Strancar, 2003). This technique was combined with transmission electron microscopy (TEM), which has been widely employed to characterize the size and shape of metal nanoparticles. SEC uses porous packing materials for separation in a column. Separation results from the distribution of the sample between the moving and stagnant mobile phase retained within the pores of the stationary phase (Teraoka, 2004). Retention time is controlled by the extent to which different fractions of the sample diffuse through the porous structure of stationary phase, which depends on the ratio of molecular dimensions to the distribution of pore size. Large molecules (particles) never enter the stationary phase and thus move quickly through the void volume of the column, whereas small molecules enter the pores of the stationary phase retarding thus their movement in the order of decreasing molecular size. This elution order is opposite to that of field-flow fractionation. Furthermore, SEC needs the addition of electrolyte for defined separation conditions. Magnetic properties are typically characterized by magnetometer measurements and Mössbauer spectroscopy.

Recently, we have reported on the development of magnetic polymer microspheres containing various iron oxide nanoparticles including those stabilized with dextran (Horák, Semenyuk, & Lednický, 2003; Horák & Benedyk, 2004). Such materials can immobilize antibodies and find applications mainly in biotechnology. The aim of this report is to elucidate some aspects associated with the colloidal stability of dextran-modified iron oxides and to contribute to thorough characterization of such colloids. The advantage of SEC consists in its ability to distinguish free dextran from both dextran-modified and unmodified iron oxide nanoparticles.

2. Experiments

2.1. Materials

Macroporous poly(glycidyl methacrylate-*co*-ethylene dimethacrylate) (poly(GMA-EDMA); 60/40, v/v) particles, ca. 7 μm in diameter, were used as a starting material for the preparation of chromatographic packing (Švec, Hradil, Kálal, & Čoupek, 1975). $K_3PO_4{\cdot}7H_2O$ was purchased from Lach-Ner, Neratovice, Czech Republic. Dextran 10, 20, T40, T70, 110, T250, T500 and 2000 were products of Pharmacia, Uppsala, Sweden. Dextran S40 was from Dextran Products Ltd., Scarborough, Canada. Other chemicals were from Sigma-Aldrich, Prague (Czech Republic) and used as received.

2.2. Preparation of iron oxide nanoparticles

Two methods have been used for the preparation of dextran-modified iron oxide nanoparticles.

2.2.1. Method A

A solution of $FeCl_2$ (0.2 mol/L) and $FeCl_3$ (0.2 mol/L) in the 1:2 molar ratio was coprecipitated in an excess of 0.5 mol/L NH_4OH. After 15 min, the product was repeatedly separated in magnetic field (permanent FeNdB magnet, coercivity ≥868 kA/m; remanence 1.2 T) and washed with Q-water to reach peptization. The colloid was subsequently sonicated for 5 min (Ultrasonic Homogenizer 4710 Series, Cole-Palmer Instruments, USA, 40% output) and oxidized with 5 wt.% NaOCl solution in the presence of sodium citrate. Washing and sonication were then repeated. Finally, 20 wt.% aqueous dextran S40 solution was added to the colloidal iron oxide (maghemite, γ-Fe_2O_3). Its structure was confirmed by Mössbauer spectroscopy (Pollert et al., 2006).

2.2.2. Method B

Ten millilitres of 5, 25 and 50 wt.% aqueous dextran S40 solution was mixed under stirring with 10 mL of an aqueous solution containing 1.51 g $FeCl_3{\cdot}6H_2O$ and 0.64 g $FeCl_2{\cdot}4H_2O$. Fifteen microlitres of 7.5% NH_4OH solution was added dropwise, until pH 12 was reached and the solution was heated to 60 °C for 15 min. Large agglomerates were destroyed by sonication for 5 min. The particles were washed by dialysis against water, using a molecular weight cut-off 14,000 Visking membrane (Carl Roth GmbH, Germany) at room temperature for 24 h, changing water 5 times until pH 6 was reached.

2.3. Preparation and characterization of adsorbent for SEC

The adsorbent for the chromatographic column was prepared by acid-hydrolysis of macroporous poly(GMA-EDMA) beads with 0.1 M H_2SO_4 at 100 °C for 1 h. The course of hydrolysis of oxirane groups was monitored by IR spectroscopy. After hydrolysis, the peak area characteristic of oxirane groups at 908 cm^{-1} disappeared.

2.4. Size-exclusion chromatography

Size-exclusion chromatography was used for characterization of the dextran-modified iron oxide. A suspension of hydrolyzed macroporous poly(GMA-EDMA) beads was packed in a 250 mm × 4 mm i.d. stainless steel column using a high-pressure pump. Elution characteristics of iron oxide

Table 1
Retention time of dextranes

Dextran	M_w[a] × 10^5	M_w[b] × 10^5	n[c]	t[d] (min)
2000	20	20	11101	2.13
T500	5	5.16	2864	2.16
T250	2.5	2.40	1332	2.67
110	1.1	1.005	558	2.81
T70	0.7	0.695	386	3.01
T40	0.4	0.420	233	3.05
20	0.2	0.223	124	3.24
10	0.1	0.093	52	3.41
Glucose	–	180.16	1	4.41

[a] Molecular weight determined by light scattering.
[b] Molecular weight by HPLC.
[c] Number of glucose units.
[d] Retention time.

nanoparticles were determined with a liquid chromatograph consisting of gradient pump model 2249 (LKB, Bromma, Sweden), differential refractometer RIDK 102 (Laboratorní přístroje, Prague, Czech Republic) and intermediate injector (Rheodyne 7725, Rheodyne, Catati, USA) equipped with a fixed 20-μL loop. The flow rate of 0.1 M K_3PO_4 in degassed water as eluent was 0.5 mL/min. Chromatography Station for Windows (CSW) software was used for the determination of chromatographic characteristics. The column was calibrated with dextrans of various molecular weights (Table 1).

2.5. Other characterization methods

The particle hydrodynamic diameter was measured by dynamic light scattering (DLS) with Autosizer Lo-C (Malvern Instruments Ltd., Malvern, Great Britain) providing z-average diameter and the polydispersity as a measure of the distribution width.

For transmission electron microscopy (TEM; JEOL JEM 200 CX), an iron oxide nanoparticle dispersion in water was sprayed on a grid with carbon membrane. The number-average nanoparticle size was determined by the measurement of at least 300 particles for each batch from the microphotographs using the Atlas program (Tescan, Digital Microscopy Imaging, Brno, Czech Republic). The number-average particle radius (r_n) was calculated, where $r_n = \Sigma r_i/N$ and N is the number of particles.

The dextran and iron oxide contents were respectively calculated from elemental analysis (Perkin-Elmer 2400 CHN, Beaconsfield, UK) and from the iron content analyzed by AAS (Perkin-Elmer 3110) of an extract from the sample obtained with dilute HCl (1:1) at 80 °C for 1 h.

IR spectra of dextran were measured by KBr technique and diffusion reflectance spectrum of dextran–iron oxide particles was measured on an FTIR spectrometer Paragon 1000PC (Perkin-Elmer).

3. Results and discussion

Dextran-modified superparamagnetic iron oxide nanoparticles were prepared by two methods: iron oxide was precipitated in a dextran solution or a dextran solution was added after alkaline precipitation. The effect of the dextran/iron oxide ratio used in the preparation on the particle morphology was investigated. Size-exclusion chromatography, transmission electron microscopy (TEM), dynamic light scattering (DLS), elemental analysis and IR spectra characterized the prepared particles. Characteristic vibrations of CH and C–O–C groups at 2900 cm^{-1} and 1300 cm^{-1}, respectively, were found in dextran-coated iron oxide nanoparticles by diffusion reflectance spectroscopy. The same bands were found in IR spectrum of dextran measured by KBr technique (Fig. 1). Diffusion reflectance spectra of the particles thus confirmed the presence of dextran on the iron oxide nanoparticle surface. The amount of dextran on the surface decreased with increasing amount of iron oxide.

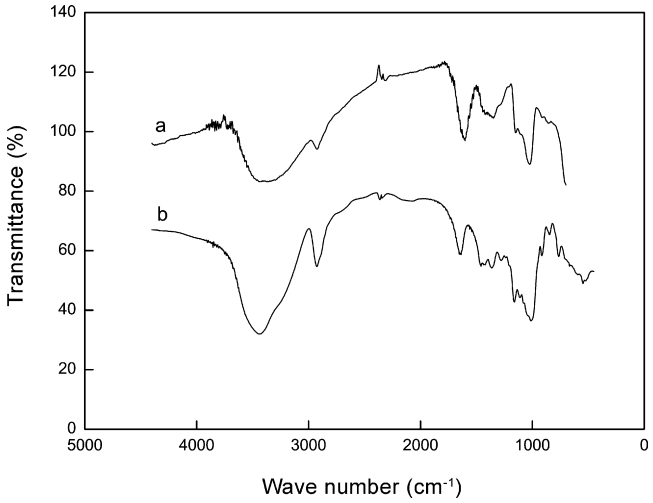

Fig. 1. Diffusion reflectance spectra of (a) dextran-modified iron oxide nanoparticles and (b) IR-spectra of dextran S40 measured by KBr technique.

3.1. Characterization of iron oxide nanoparticles by size-exclusion chromatography

Nanoparticle behaviour and changes in the colloid composition during storage were determined by size-exclusion chromatography. The packed column was calibrated with glucose and dextrans showing a good range of separation for molecular weights 10,000–2,000,000. The chromatograms (Figs. 2 and 3) confirmed that the separation not only of dextran, but also of iron oxide nanoparticles was consistent with the size-exclusion mechanism. The peak areas also reflected dextran and dextran-modified iron oxide particle concentrations; other peaks corresponded to NH_4Cl and air. Dextran and iron oxide particles can be distinguished by the peak response of iron oxide nanoparticles in refractive index detector opposite to that of NH_4Cl and air. Two peaks on chromatogram indicated two types of iron oxide particles: dextran-modified iron oxide clusters (Fig. 2, peak I) and bare iron oxide nanoparticles (Fig. 2, peak II).

3.1.1. Dextran-modified iron oxide nanoparticles prepared by Method A

Method A is based on the iron oxide precipitation followed by the addition of a dextran S40 solution, which consists of

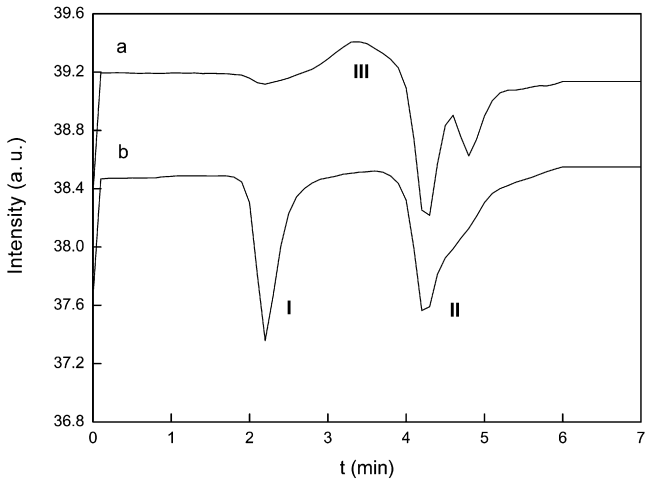

Fig. 2. Chromatograms of iron oxide nanoparticles prepared by Method A. Dextran/iron oxide: (a) 18.18 and (b) 0.154.

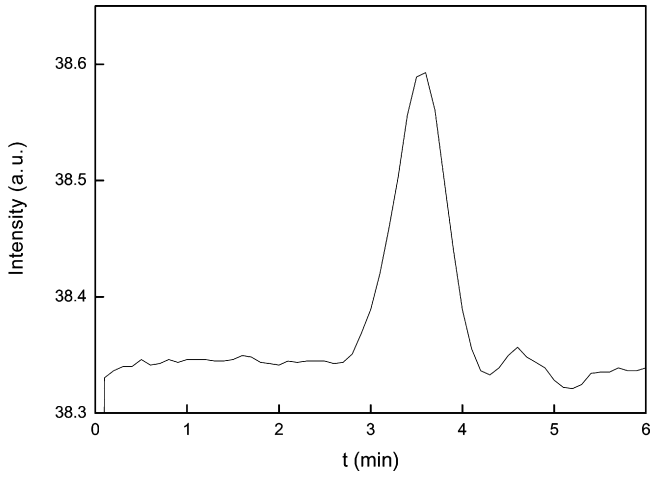

Fig. 4. Chromatogram of Dextran S40.

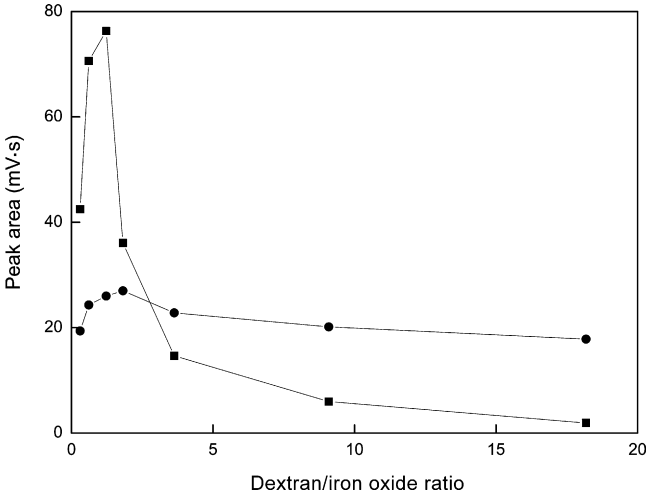

Fig. 3. Dependence of the amount of (■) dextran-modified iron oxide clusters (peak I) and (●) of primary iron oxide nanoparticles (peak II) in the colloid on the starting dextran/iron oxide ratio.

81 wt.% of dextran of molecular weight 4.1×10^4 and 19 wt.% of dextran of molecular weight 812 (Fig. 4). The effects of the starting dextran/iron oxide ratio and storage on the composition and elution time of the particles were determined.

The elemental analysis of dried colloids (Table 2) and the following calculations showed that the composition of dextran-modified superparamagnetic iron oxide nanoparticles was equal to the starting composition.

In the starting colloid without dextran and at the dextran/iron oxide ratios up to 0.16, only small primary iron oxide nanoparticles with a retention time 4.3 min were found (Table 3). If dextran was added at the dextran/iron oxide ratio of 0.31 after the iron oxide precipitation, entity with corresponding retention time 2.25 min (Table 3) was observed. The elution time of dextran-modified iron oxide entities prepared by Method A then did not change with increasing the starting dextran/iron oxide ratio from 0.31 to 18 (Table 3). These SEC-observed entities are assumed to be dextran-modified iron oxide nanoparticle clusters. Also the retention time of primary iron oxide nanoparticles equivalent to 4.3 min did not depend on the starting dextran/iron oxide ratio.

The amount of dextran-modified iron oxide nanoparticle clusters was high at low dextran/iron oxide ratios; however, it approached zero at high ratios because the clusters disintegrated (Fig. 3). In colloids prepared at the dextran/iron oxide ratios ranging from 0 to 0.16, the peak of dextran-modified iron oxide clusters was never found. Free dextran S40 was always found in colloids obtained at the dextran/iron oxide ratios higher than 0.61

Table 2
Comparison of starting and obtained dextran–iron oxide composition calculated from elemental analysis

Colloid	Starting composition	Elemental analysis			Calculated		
	Dextran/iron oxide ratio (w/w)	%C	%H	%Fe	Dextran (mg)	Iron oxide (mg)	Dextran/iron oxide ratio (w/w)
F1	0	0	0	65.13	0	208.39	0
F2	0.06	2.80	0.70	58.87	15.11	188.35	0.08
F3	0.16	5.56	0.88	59.64	30.02	190.82	0.16
F4	0.31	9.42	1.35	42.65	50.91	136.47	0.37
F5	0.61	15.52	2.77	48.09	83.85	153.88	0.54
F6	1.23	21.36	3.71	31.50	115.44	100.79	1.15
F7	1.82	25.69	4.34	21.75	138.81	69.60	1.99
F8	3.63	31.57	5.30	14.05	170.62	44.94	3.80
F9	9.09	35.97	6.31	7.06	194.40	22.59	8.61

Colloid F1 ($c = 11$ mg iron oxide/mL) was used for preparation.

Table 3
Ferrofluid nanoparticles prepared by Method A—retention time and peak area determination (immediately after preparation)

Colloid	Dextran/iron oxide ratio (mg/mg)	t (min)[a]			Peak area (mV s)		
		Peak I[b]	Peak II[c]	S40[d]	Peak I[b]	Peak II[c]	Peak III[d]
F1	0	–	4.28	–	–	28.06	–
F2	0.06	–	4.29	–	–	32.14	–
F3	0.16	–	4.31	–	–	35.38	–
F4	0.31	2.23	4.27	–	47.60	18.99	–
F5	0.61	2.26	4.26	–	74.15	21.57	–
F6	1.23	2.23	4.26	3.52	83.12	21.17	2.57
F7	1.82	2.22	4.27	3.51	39.95	24.67	5.22
F8	3.63	2.23	4.31	3.51	19.38	19.81	7.86
F9	9.09	2.23	4.32	3.52	10.80	15.26	8.53
F10	18.18	2.29	4.29	3.52	6.88	16.71	8.90

Colloid F1 (c = 11 mg iron oxide/ml) was used for preparation.
[a] Retention time.
[b] Dextran-modified iron oxide clusters.
[c] Bare iron-oxide.
[d] Dextran S40.

(Fig. 2, Peak III). In contrast, free dextran S40 never appeared in the colloids prepared at the dextran/iron oxide ratios ranging from 0 to 0.61. A high amount of iron oxide clusters was also found at the dextran/iron oxide ratio of 1.82.

Changes in the retention time of dextran-modified iron oxide nanoparticle clusters with time were observed. The retention time was prolonged after 4–5 months storage reflecting the decrease of particle cluster size. In this case, only samples with the dextran/iron oxide ratios of 1.82–18.18 contained free dextran. The amount of free dextran increased with increasing the dextran/iron oxide ratio. The changes of retention time of particle clusters with time may be explained by dextran hydrolysis (Browarzik, 1997; Confer & Logan, 1997).

3.1.2. *Dextran-modified iron oxide nanoparticles prepared by Method B*

In Method B, iron oxide was precipitated directly in 5, 25 and 50 wt.% aqueous dextran solution. In 5 wt.% dextran solution, colloidal nanoparticles were not formed, but voluminous

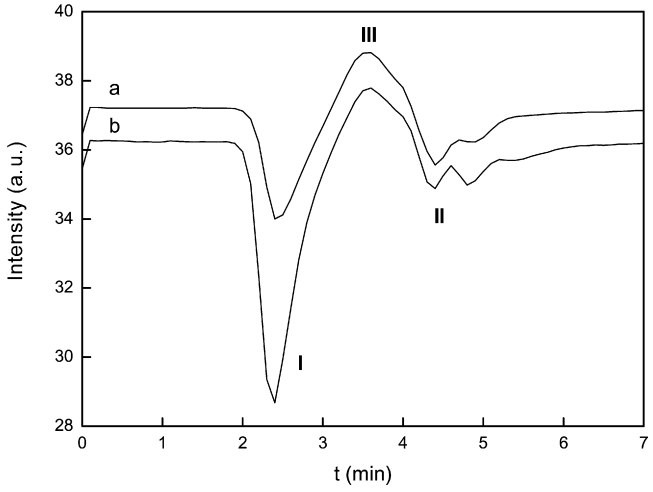

Fig. 5. Chromatograms of ferrofluid nanoparticles prepared in (a) 25 wt.% and (b) 50 wt.% dextran solution by Method B.

Table 4
Ferrofluid nanoparticles prepared by Method B by precipitation in 25 and 50 wt.% dextran solution—molecular weight and retention time evaluation

Colloid	Dialysis time (h)	t[a] (min)		
		Peak I[b]	Peak II[c]	Peak III[d]
N5-25[e]	25	2.41	4.43	3.65
N6-25[e]	49	2.39	4.36	3.51
N7-25[e]	122.5	2.45	4.33	3.47
N8-25[e]	147.5	2.43	4.44	3.48
N1-50[f]	48	2.47	4.47	3.61
N2-50[f]	70	2.51	4.37	3.52
N3-50[f]	144	2.41	4.39	3.48
N4-50[f]	166	2.51	4.37	3.49

[a] Retention time.
[b] Dextran-modified iron oxide clusters.
[c] Bare iron-oxide.
[d] Dextran S40.
[e] Dextran 25 wt.%.
[f] Dextran 50 wt.%.

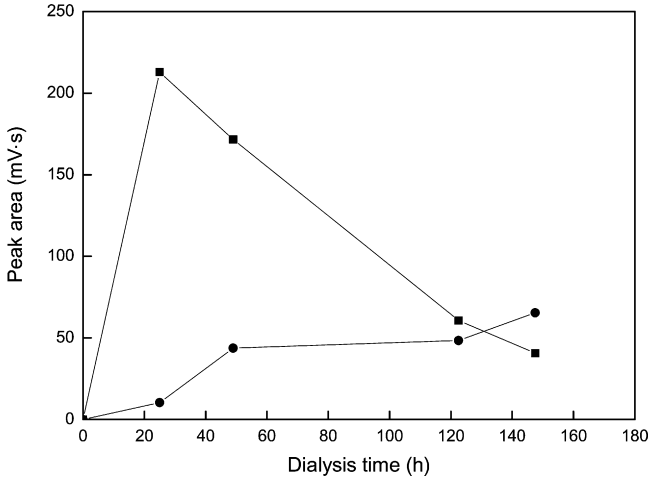

Fig. 6. Dependence of the amount of (●) dextran (peak III) and (■) dextran-modified iron oxide nanoparticle clusters (peak I) on dialysis time using Visking membrane. Colloid was prepared in 25 wt.% dextran solution by Method B.

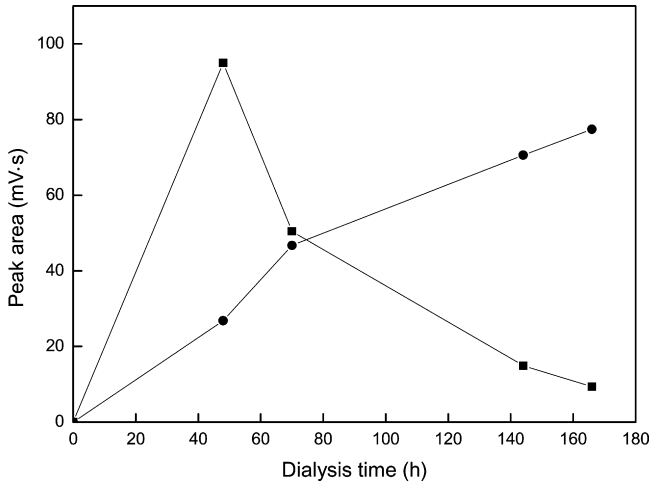

Fig. 7. Dependence of the amount of (●) dextran (peak III) and (■) dextran-modified iron oxide nanoparticle clusters (peak I) on dialysis time using Visking membrane. Colloid was prepared in 50 wt.% dextran solution.

amorphous sediment. The results from size exclusion chromatography are shown in Table 4 and Figs. 5–7. The peak of free dextran S40 (peak III in Fig. 5) was observed in all three sets of experiments employing 5, 25 and 50 wt.% dextran solution. To purify the synthesized iron oxide colloid, the dispersion was dialyzed. With increasing dialysis time, the retention time of both dextran-modified iron oxide clusters and primary iron oxide nanoparticles almost did not change (Table 4). The average retention time of dextran-modified iron oxide nanoparticle clusters prepared in 25 and 50 wt.% dextran solution was 2.42 and 2.48 min, respectively. The amount of dextran-modified iron oxide nanoparticle clusters was high at short dialysis time (Figs. 6 and 7). With increasing dialysis time, the amount of clusters decreased and free dextran was found. After 150 h dialysis, the amount of clusters was one tenth of the maximal value for precipitation in 25 wt.% dextran solution and one sixth for precipitation in 50 wt.% dextran solution. It can thus be concluded that an increase in dialysis time induced the disintegration of dextran-modified iron oxide clusters.

3.2. Determination of iron oxide radius by TEM and DLS

Fig. 8 shows the TEM micrograph of dextran-modified iron oxide nanoparticles prepared by Method A. Their shape was not strictly spherical, but it could be approximated by spheres for the purpose of particle size determination by image analysis. The dependence of the dextran-modified iron oxide particle size on the starting dextran/iron oxide ratio was not conclusive (Fig. 9) with the radius in the range 3–5 nm (according to TEM).

The hydrodynamic size of the particles was measured by dynamic light scattering as a function of the dextran/iron oxide ratio (Fig. 9). The particle radius increased from 46 to 62 nm if the dextran/iron oxide ratio increased from 0 to 3.6 before reaching a plateau at the ratios higher than 3.6. The size measured by DLS is that of water-swollen particles (hydrodynamic radius), whereas the size deduced from TEM measurement corresponds to particles in a dried state. Therefore the particle size from TEM measurements in a dried state cannot be compared

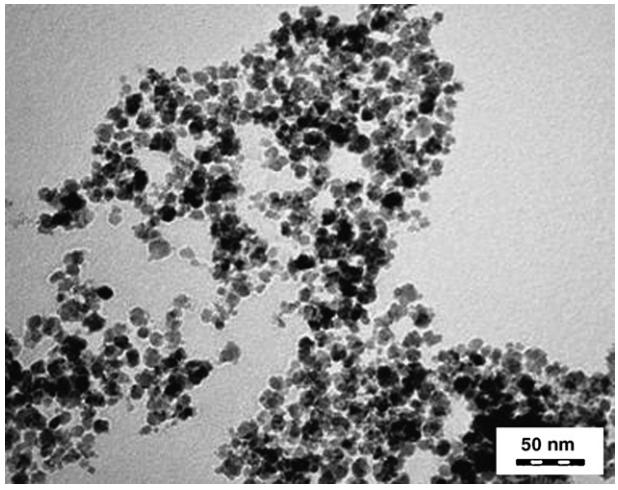

Fig. 8. TEM micrograph of dry colloid F4.

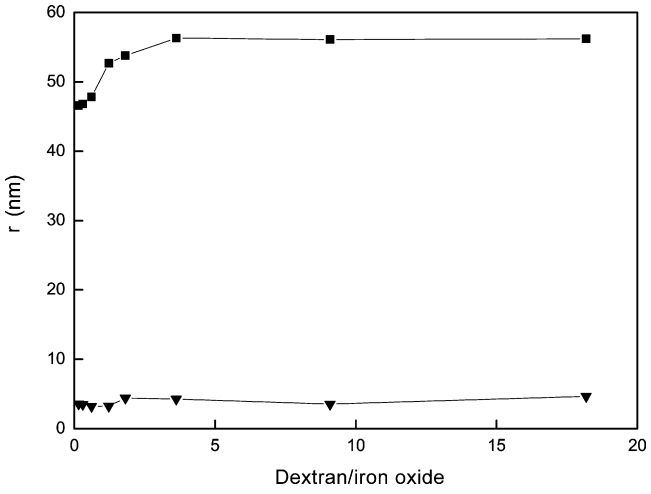

Fig. 9. Comparison of particle radius determined by (■) dynamic light scattering and (▼) transmission electron microscopy.

with the values from DLS measurements and DLS gave higher values compared to TEM. This can also be ascribed to the effect of large particles on hydrodynamic radius, because the DLS provides *z*-average of the radius. Any other reason can consist in that modified iron oxide particles are slightly aggregated in water. The difference in the mean sizes obtained by DLS and electron microscopy has already been observed with other materials (Bootz, Vogel, Schubert, & Kreuter, 2004), possibly due to the hydrophilic polymer coating of the particles which increases significantly the hydrodynamic radius, especially with very small colloids, but which is fully collapsed in the dried state.

4. Conclusions

Dextran-modified iron-oxide nanoparticles were prepared by two methods, namely precipitation of iron salts in the presence of dextran solution, or the dextran solution was added after precipitation. Size-exclusion chromatography, dynamic light scattering and transmission electron microscopy characterized the prepared colloids. Size-exclusion chromatography made possible

the determination of free dextran and subsequent concentration changes with storage time. Peak of dextran-modified iron oxide clusters was never found in colloids prepared by Method A at the dextran/iron oxide ratio ranging from 0 to 0.16. Free dextran S40 was found in colloids obtained at the dextran/iron oxide ratio higher than 0.61, but it never appeared in the colloids prepared at the dextran/iron oxide ratio ranging from 0 to 0.61. Only small nanoparticles with a retention time 4.3 min were found in the starting ferrofluid. If the dextran/iron oxide ratio was higher than 0.16, nanoparticle clusters with a typical retention time 2.25 min were found. The retention time of clusters of particles prepared by Method A increased with the storage time. When the dextran-modified nanoparticles were prepared by Method B, the retention time of clusters was about 2.4 min.

Dextran-modified iron-oxide nanoparticles are intended for biomedical applications. In the ferrofluids prepared by Method B in 5–50 wt.% dextran solution, the peak of free dextran was found. That disqualifies such particles from biomedical applications. SEC results showed that the initial dextran/iron oxide ratio is the effective parameter to control the nanoparticle size as reflected in changes of retention time. The dextran/iron oxide ratio 0–0.16 used in Method A can be recommended for synthesis of particles that could be suitable for biomedical applications, as the colloid does not contain excessive dextran or iron oxide clusters.

Acknowledgment

Financial support of the Grant Agency of the Czech Republic project no. 203/05/2256 is gratefully acknowledged.

References

Anger, S., Caldwell, K., Mehnert, W., & Muller, R. (1999). Coating of nanoparticles: Analysis of adsorption using sedimentation field-flow fractionation (SdFFF). *Proceedings of International Symposium of Controlled Release of Bioactivated Materials*, *26*, 599–600.

Bonnemain, B. (1998). Superparamagnetic agents in magnetic resonance imaging: Physicochemical characteristics and clinical applications—A review. *Journal of Drug Targeting*, *6*(3), 167–174.

Bootz, A., Vogel, V., Schubert, D., & Kreuter, J. (2004). Comparison of scanning electron microscopy, dynamic light scattering and analytical ultracentrifugation for the sizing of poly(butyl cyanoacrylate) nanoparticles. *European Journal of Pharmaceutics and Biopharmaceutics*, *57*(2), 369–375.

Browarzik, D. (1997). Continuous kinetics of dextran degradation. *Journal of Macromolecular Science Pure and Applied Chemistry*, *34*(3), 397–404.

Cabasso, I., & Yuan, Y. (1996). Nanoparticles in polymer and polymer dendrimers. In J. Fendler & I. Dekany (Eds.), *NATO ASI Series. Part 18 Nanoparticles in Solids and Solutions* (pp. 131–153).

Chastellain, M., Petri, A., & Hofmann, H. (2004). Particle size investigation of a multistep synthesis of PVA coated superparamagnetic nanoparticles. *Journal of Colloid Interface Science*, *278*(2), 353–360.

Chmela, E., Tijssen, R., Blom, M. T., Gardeniers, H. J. G. E., & van den Berg, A. (2002). A chip system for size separation of macromolecules and particles by hydrodynamic chromatography. *Analytical Chemistry*, *74*(14), 3470–3475.

Confer, D. R., & Logan, B. E. (1997). Molecular weight distribution of hydrolysis product during the biodegradation of model macromolecules in suspended and biofilm cultures. II: Dextran and dextrin. *Water Research*, *31*(9), 2137–2145.

Griffiths, C. H., O'Horo, M. P., & Smith, T. W. (1979). The structure, magnetic characterization and oxidation of colloidal iron dispersions. *Journal of Applied Physics*, *50*(11), 7108–7115.

Gupta, A. K., & Gupta, M. (2005). Synthesis and surface engineering of iron oxide nanoparticles for biomedical applications. *Biomaterials*, *26*(18), 3995–4021.

Horák, D., & Benedyk, N. (2004). Magnetic poly(glycidyl methacrylate) microspheres prepared by dispersion polymerization in the presence of electrostatically stabilized ferrofluids. *Journal of Polymer Science Part A: Polymer Chemistry*, *42*(22), 5827–5837.

Horák, D., Semenyuk, N., & Lednický, F. (2003). Effect of the reaction parametrs on the particle size in the dispersion polymerization of 2-hydroxyethyl and glycidyl methacrylate in the presence of a ferrofluid. *Journal of Polymer Science Part A: Polymer Chemistry*, *41*(12), 1848–1863.

Janča, J., Ananieva, I. A., Menshikova, A. Y., & Evseeva, T. G. (2004). Micro-thermal focusing field-flow fractionation. *Journal of Chromatogry B*, *800*(1–2), 33–40.

Janča, J., Berneron, J.-F., & Boutin, R. (2003). Micro-thermal field-flow fractionation: New high performance method for particle size distribution analysis. *Journal of Colloid Interface Science*, *260*(2), 317–323.

Janča, J., & Strnad, P. (2004). Micro and frontal thermal field-flow fractionation: On the shear degradation of ultra-high molar mass polymers. *Journal of Liquid Chromatography Related Technology*, *27*(2), 193–214.

Johann, C. (1998). Asymmetrical field flow fractionation for polymer and particle characterization. *GIT Labor-Fachzeitschrift*, *42*, 119–120.

Jolivet, J. P., Massart, R., & Fruchart, J. M. (1983). Synthesis and physicochemical study on nonsurfactant magnetic colloids in aqueous medium. *Nouveau Journal De Chimie—New Journal of Chemistry*, *7*(5), 325–331.

Kaminski, M. D., & Rosengart, A. J. (2005). Detoxification of blood using injectable magnetic nanospheres: A conceptual technology description. *Journal of Magnetism and Magnetic Materials*, *293*(1), 398–403.

Kramberger, P., Glover, D., & Strancar, A. (2003). Application of monolithic columns for the fast separation of nanoparticles. *American Biotechnology Laboratory*, *21*(13), 27–28.

Liu, F., & Wei, G. (2004). Effect of mobile-phase additives on separation of gold nanoparticles by size-exclusion chromatography. *Chromatographia*, *59*(1–2), 115–119.

Massart, R. (1981). Preparation of aqueous magnetic liquids in alkaline and acidic media. *IEEE Transaction on Magnetization*, *17*(2), 1247–1248.

Molday, R. S. (1984). *Magnetic iron oxide microspheres*. U.S. Patent 4,452, 773.

Moon, M. H. (2001). Frit-inlet asymmetrical flow field-flow fractionation (FI-AFlFFF): A stopless separation technique for macromolecules and nanoparticles. *Bulletin of Korean Chemical Society*, *22*(4), 337–348.

Neuberger, T., Schöpf, B., Hofmann, H., Hofmann, M., & von Rechenberg, B. M. (2005). Superparamagnetic nanoparticles for biomedical applications: Possibilities and limitations of a new drug delivery system. *Journal of Magnetism and Magnetic Materials*, *293*(1), 483–496.

Papel, S. S. (1965). *Low viscosity magnetic fluid obtained by the colloidal suspension of magnetic particles*. U.S. Patent 3,215,572.

Pollert, E., Knížek, K., Maryško, M., Závěta, K., Lančok, A., Boháček, J., et al. (2006). Magnetic poly(glycidyl methacrylate) microspheres containing maghemite prepared by emulsion polymerization. *Journal of Magnetism and Magnetic Materials*, *306*, 241–247.

Rheinlander, T., Roessner, D., Weitschies, W., & Semmler, W. (2000). Comparison of size-selective techniques for the fractionation of magnetic fluids. *Journal of Magnetism and Magnetic Materials*, *214*(3), 269–275.

Švec, J., Hradil, J., Kálal, F., & Čoupek, J. (1975). Reactive polymers. I. Macroporous methacrylate copolymers containing epoxy groups. *Angewandte Makromolekulare Chemie*, *48*, 135–143.

Syirkin, V. G., & Polushina, N. E. (1967). Preparation of finely dispersed uniform powder of iron oxide using carbonyl technique. *Poroshk. Metallurgy*, *4*, 1–7.

Teraoka, I. (2004). Calibration of retention volume in size exclusion chromatography by hydrodynamic radius. *Macromolecules*, *37*(17), 6632–6639.

Wei, G., Liu, F. K., & Wang, C. R. C. (1999). Shape separation of nanometer gold particles by size-exclusion chromatography. *Analytical Chemistry*, *71*(11), 2085–2091.

Williams, A., Varela, E., Meehan, E., & Tribe, K. (2002). Characterization of nanoparticulate systems by hydrodynamic chromatography. *International Journal of Pharmaceutics B*, *242*, 295–299.